Oncogene
https://doi.org/10.1038/s41388-019-1086-x

ARTICLE

A CD133-AKT-Wnt signaling axis drives glioblastoma brain tumor-initiating cells

Branavan Manoranjan[1,2,3] · Chirayu Chokshi[2,3] · Chitra Venugopal[2] · Minomi Subapanditha[2] · Neil Savage[2] · Nazanin Tatari[2,3] · John P. Provias[4] · Naresh K. Murty[5] · Jason Moffat[6] · Bradley W. Doble[2,3] · Sheila K. Singh[2,3,5]

Received: 12 May 2018 / Revised: 23 October 2019 / Accepted: 25 October 2019

Abstract

Mechanistic insight into signaling pathways downstream of surface receptors has been revolutionized with integrated cancer genomics. This has fostered current treatment modalities, namely immunotherapy, to capitalize on targeting key oncogenic signaling nodes downstream of a limited number of surface markers. Unfortunately, rudimentary mechanistic understanding of most other cell surface proteins has reduced the clinical utility of these markers. CD133 has reproducibly been shown to correlate with disease progression, recurrence, and poor overall survivorship in the malignant adult brain tumor, glioblastoma (GBM). Using several patient-derived $CD133^{high}$ and $CD133^{low}$ GBMs we describe intrinsic differences in determinants of stemness, which we owe to a CD133-AKT-Wnt signaling axis in which CD133 functions as a putative cell surface receptor for AKT-dependent Wnt activation. These findings may have implications for personalized oncology trials targeting PI3K/AKT or Wnt as both pathways may be activated independent of their canonical drivers, leading to treatment resistance and disease relapse.

Introduction

Contemporary frameworks for studying tumorigenesis consider the process as development gone awry. Cell surface markers have traditionally been used to characterize the continuum of cellular phenotypes generated in ontogeny and carried forward into oncology as tumor-initiating cells (TICs). CD133 was originally identified as a marker of self-renewing hematopoietic [1] and neural stem cell [2] populations. Subsequently, it has been used to characterize cells capable of tumor initiation and maintenance in a variety of human cancers [3–6], including the most malignant adult brain tumor, glioblastoma (GBM) [6]. With few markers of clinical utility in adult GBM, CD133 has reproducibly been shown to correlate with disease progression, recurrence, and poor overall survivorship [7, 8] but insight into its function remains limited. Given the activation of AKT signaling in ~50% of GBMs secondary to EGFR amplification and/or overexpression, activating mutations in PI3K, or inactivating mutations in PTEN [9], emerging studies have suggested CD133 to function as a novel receptor for the PI3K/AKT pathway [10]. Although CD133 is the first identified member of the Prominin family of pentaspan membrane glycoproteins, with an implied role in cell signaling, the mechanism by which it regulates stemness to bridge developmental and oncogenic cellular programs has not yet been described.

The Wnt signaling pathway promotes the expansion of neural stem cells (NSCs) in the forebrain during fetal development [11, 12] and its components, namely β-catenin, are persistently overexpressed in GBM [13, 14]. Interestingly, unlike colorectal cancer or pediatric

Supplementary information The online version of this article (https://doi.org/10.1038/s41388-019-1086-x) contains supplementary material, which is available to authorized users.

✉ Sheila K. Singh
ssingh@mcmaster.ca

1 Michael G. DeGroote School of Medicine, McMaster University, Hamilton, ON L8S 4K1, Canada

2 McMaster Stem Cell and Cancer Research Institute, McMaster University, Hamilton, ON L8S 4K1, Canada

3 Departments of Biochemistry and Biomedical Sciences, McMaster University, 1200 Main Street West, Hamilton, ON L8N 3Z5, Canada

4 Departments of Pathology, McMaster University, 1200 Main Street West, Hamilton, ON L8N 3Z5, Canada

5 Surgery, Faculty of Health Sciences, McMaster University, 1200 Main Street West, Hamilton, ON L8N 3Z5, Canada

6 The Donnelly Centre, University of Toronto, Toronto, ON M5S 3E1, Canada

Published online: 06 November 2019

medulloblastoma in which elevated β-catenin expression is attributed to stabilizing mutations in *CTNNB1* [15] or inactivating mutations in APC [16], GBM has not been shown to contain recurrent mutations in the Wnt pathway [9, 17–25]. With recent data independently illustrating CD133-mediated [15] or AKT-dependent [26] activation of β-catenin, a context-dependent cross-talk pathway may be implicated in the overexpression of β-catenin seen in GBM.

We have used several primary patient-derived CD133^{high} and CD133^{low} GBM lines to describe intrinsic differences in determinants of stemness. With the aim of identifying the cellular machinery that drives self-renewal downstream of CD133, we have used small molecule inhibitors that target several components of this pathway. The use of Wnt reporters has enabled us to further illustrate a mechanism by which CD133 may contribute to the genetic and phenotypic diversity seen in GBM. Our work establishes a CD133-AKT-Wnt signaling axis in which CD133 functions as a putative cell surface receptor for AKT-dependent activation of Wnt signaling. These findings may have implications for personalized oncology trials targeting PI3K/AKT or Wnt as both pathways may be activated independent of their canonical drivers, leading to treatment resistance, disease relapse, and poor overall survival.

Results

CD133^{high} GBMs contain elevated levels of endogenous Wnt activity when compared with CD133^{low} GBMs

As recent single-cell sequencing studies have highlighted the immense level of genetic and phenotypic diversity present in GBM [27, 28], we initially screened our GBM BTIC lines to assess the variability in CD133 cell surface protein expression (Supplementary Fig. 1). In keeping with the current literature on cellular diversity in GBM [27, 28], our samples displayed a range in their CD133 expression from elevated levels similar to those observed in NSCs to near negligible values (Fig. 1a). As established in recent literature, CD133 expression in our samples correlated with their self-renewal potential (Supplementary Fig. 2). To determine the extent of downstream Wnt activation, we measured endogenous levels of Wnt pathway activity using the TCF reporter assay. Wnt reporter activity closely resembled the trend observed with CD133 expression, as BTIC lines either contained elevated Wnt levels mirroring those in NSCs or displayed very minimal reporter activity (Fig. 1b). These results were validated with *Axin2* transcript expression (Fig. 1c). To appreciate the marked difference in downstream Wnt activation based on CD133 cell surface expression, we compared TCF reporter activity (Fig. 1d) and *Axin2* expression (Fig. 1e) in CD133^{high} and CD133^{low} BTIC lines. Both comparisons yielded a significant enrichment in overall Wnt pathway activation in CD133^{high} GBMs compared with CD133^{low} samples. These findings support a correlative effect on stemness in a subset of GBMs where both CD133 and the Wnt pathway are enriched to maintain a BTIC state.

CD133 activates Wnt/β-catenin signaling through AKT

In order to validate the functional significance of CD133 as a modulator of stemness, we generated stable BTIC lines by ectopically expressing CD133 in BTICs with negligible levels of CD133 on the cell surface (Supplementary Fig. 3a). A significant increase in the proliferative (Fig. 2a) and self-renewal (Fig. 2b, Supplementary Fig. 3b) potentials were observed following CD133 overexpression. To determine the effect of CD133 expression on endogenous Wnt activity, we compared TCF reporter levels in control and CD133 overexpressed samples and noted a significant increase in Wnt reporter activity with CD133 overexpression (Fig. 2c). With the surmounting evidence in support of a functional and mechanistic association between CD133 and AKT in gliomas [10, 29–31], little work has been done to understand the process by which this interaction may promote a BTIC phenotype. Given that activated AKT may phosphorylate GSK-3 on Ser9 [32], leading to the inactivation of GSK-3, we surmised that AKT-dependent β-catenin stabilization may drive downstream Wnt signaling and promote self-renewal in GBM. Western blots of multiple BTIC lines comparing control and CD133 overexpression identified a marked increase in pAKT (Ser473), pGSK-3 (Ser9), and β-catenin following CD133 overexpression (Fig. 2d). In fact, the treatment of BTICs with WNT inhibitor XAV939 led to an opposite trend, with decreases observed in pAKT (Ser473) and surface CD133 surface expression (Fig. 2e, f). Therefore, while CD133 may promote the proliferation and self-renewal of BTICs, this process may be through a novel context-specific Wnt pathway activation through AKT.

Inhibition of CD133 or AKT impairs downstream Wnt activity in BTICs

To further characterize the CD133-AKT-Wnt signaling axis, we targeted both CD133 (Supplementary Fig. 4a, b) and AKT (Supplementary Fig. 4c, d) with small molecule inhibitors and assessed their downstream effects on Wnt signaling. By using RW03, a novel anti-CD133 monoclonal antibody, we have been able to further validate CD133 as a putative functional BTIC surface receptor. Treatment with RW03 resulted in down regulation of surface CD133 expression (Fig. 3a, Supplementary Fig. 5), self-renewal

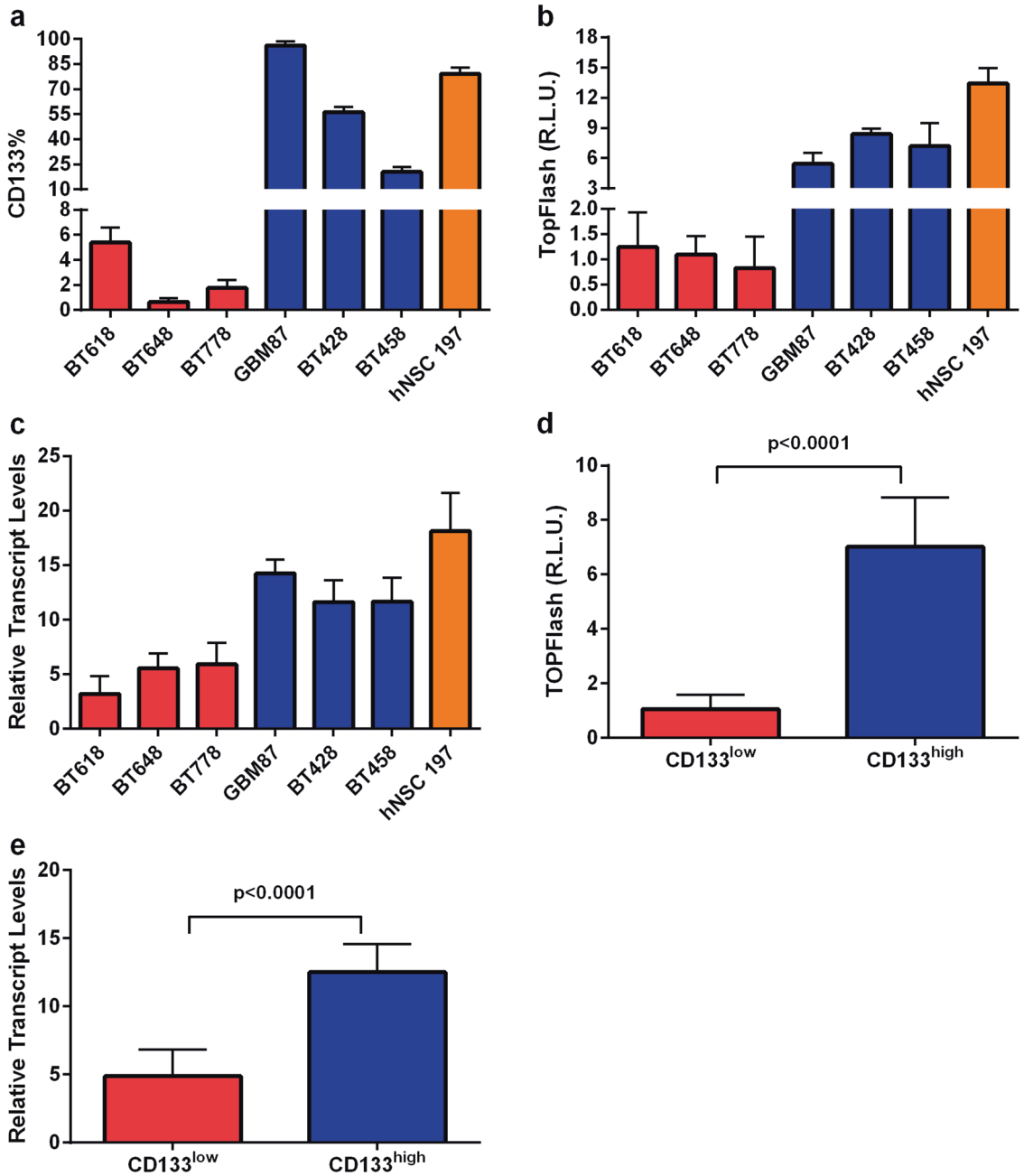

Fig. 1 CD133 expression correlates with Wnt activity in GBM. GBMs display differential CD133 cell surface protein expression ($n = 3$, independent experiments per GBM line). **b** TCF reporter analysis identifies GBMs with low and high endogenous Wnt activity ($n = 3$, independent experiments per GBM line). **c** *Axin2* is differentially expressed across several GBM samples ($n = 3$, independent experiments per GBM line). $CD133^{high}$ ($n = 3$) GBMs have higher **d** TCF reporter activity ($p < 0.0001$) and **e** *Axin2* transcript levels ($p < 0.0001$, all samples normalized to *GAPDH*) when compared with $CD133^{low}$ GBMs ($n = 3$)

potential (Fig. 3b), and a significant decrease in TCF reporter activity (Fig. 3c) in multiple independent BTIC lines when compared with controls. We then assessed the functional and mechanistic effects of AKT inhibition on GBM BTICs. Treatment with the small molecule pan-AKT inhibitor, MK-2206, reduced the proliferative (Fig. 3d) and self-renewal capacity (Fig. 3e) of $CD133^{hi}$ BTICs. In fact, self-renewal capacity of BTICs with low surface CD133 expression was sensitized to AKT inhibition following ectopic CD133 expression (Supplementary Fig. 4e, f). TCF reporter assays confirmed the downstream inhibition of Wnt activity following AKT inhibition (Fig. 3f), which provided additional data in support of a context-specific role by which AKT may regulate Wnt/β-catenin signaling.

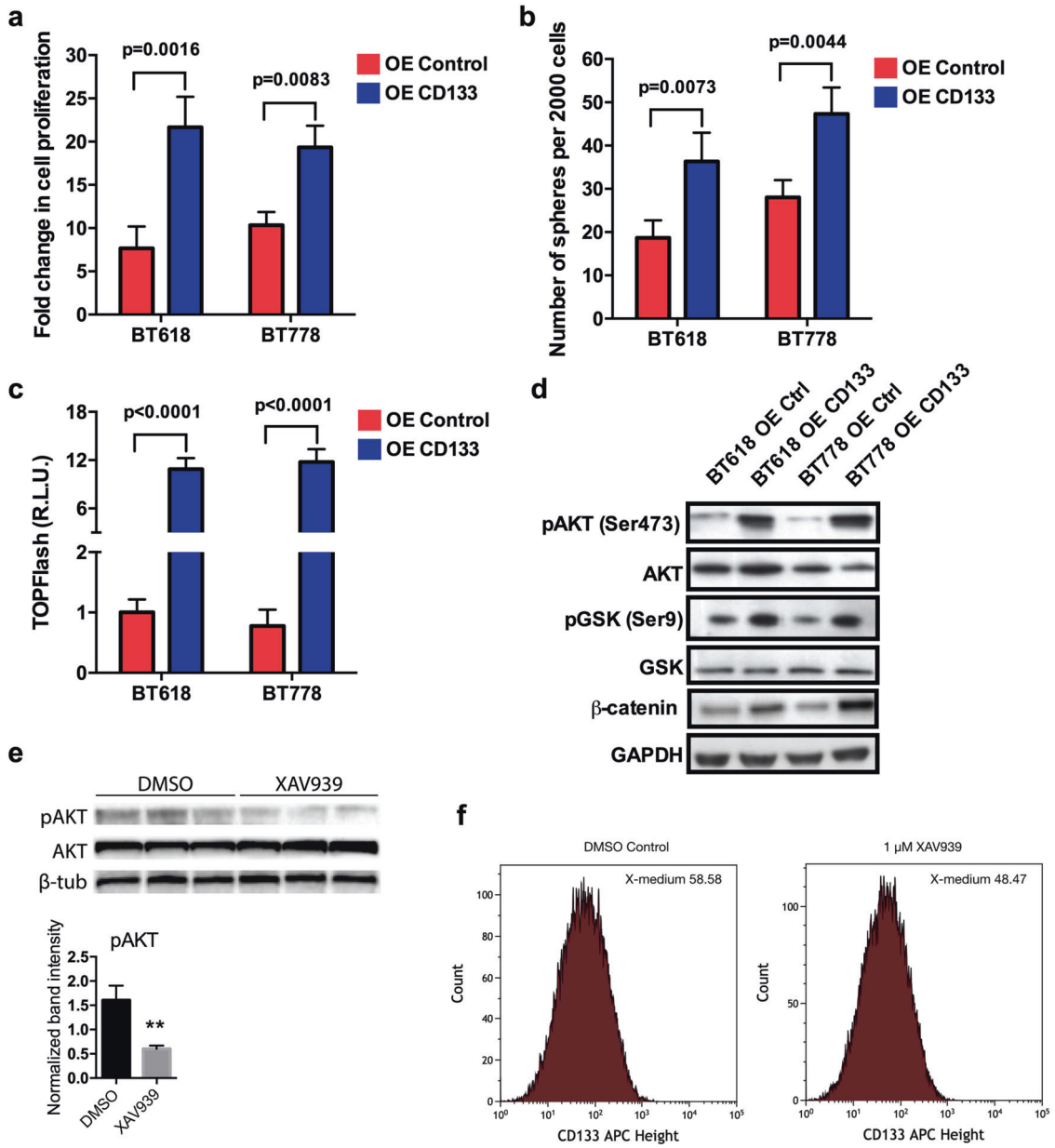

Fig. 2 CD133 regulates Wnt through AKT. **a** Proliferation (BT618: $p = 0.0016$, BT778: $p = 0.0083$) and **b** self-renewal capacity (BT618: $p = 0.0073$, BT778: $p = 0044$) of GBM cells are significantly enhanced following CD133 overexpression ($n = 3$, independent experiments per GBM line). **c** A marked increase in TCF reporter assay following CD133 overexpression indicates an increase in endogenous Wnt activity in response to CD133 overexpression (BT618: $p < 0.0001$, BT778: $p < 0.0001$, $n = 3$, independent experiments per GBM line). **d** Protein levels of putative CD133-AKT-Wnt signaling axis indicating an increase in pAKT, pGSK, and β-catenin following the ectopic expression of CD133 in two independent GBM lines ($n = 1$). **e** Protein levels of putative CD133-AKT-Wnt signaling axis indicating a decrease in pAKT after treatment of BT935 GBM BTICs with 1 μM XAV939 for 5 min ($n = 3$). **b** Flow cytometric characterization of surface CD133 levels in BT935 GBM BTICs after inhibition of Wnt signaling using 1 μM XAV939 for 24 h

GBM BTICs with endogenous Wnt activity promote tumorigenesis

Given the significant level of genetic intratumoral heterogeneity in GBM and having recognized the variable expression of CD133 and Wnt activity across several BTIC lines, we aimed to validate the functional importance of our novel CD133-AKT-Wnt signaling axis on perpetuating a malignant phenotype. After confirming endogenous CD133 expression (Supplementary Fig. 6a), BTICs were transduced with a lentiviral Wnt reporter construct (7XTCF-GFP) [33], allowing us to isolate and compare BTICs based on their endogenous levels of Wnt activation. GFP+ (referred to as TGP+) and GFP− (referred to as TGP−) cell populations were isolated

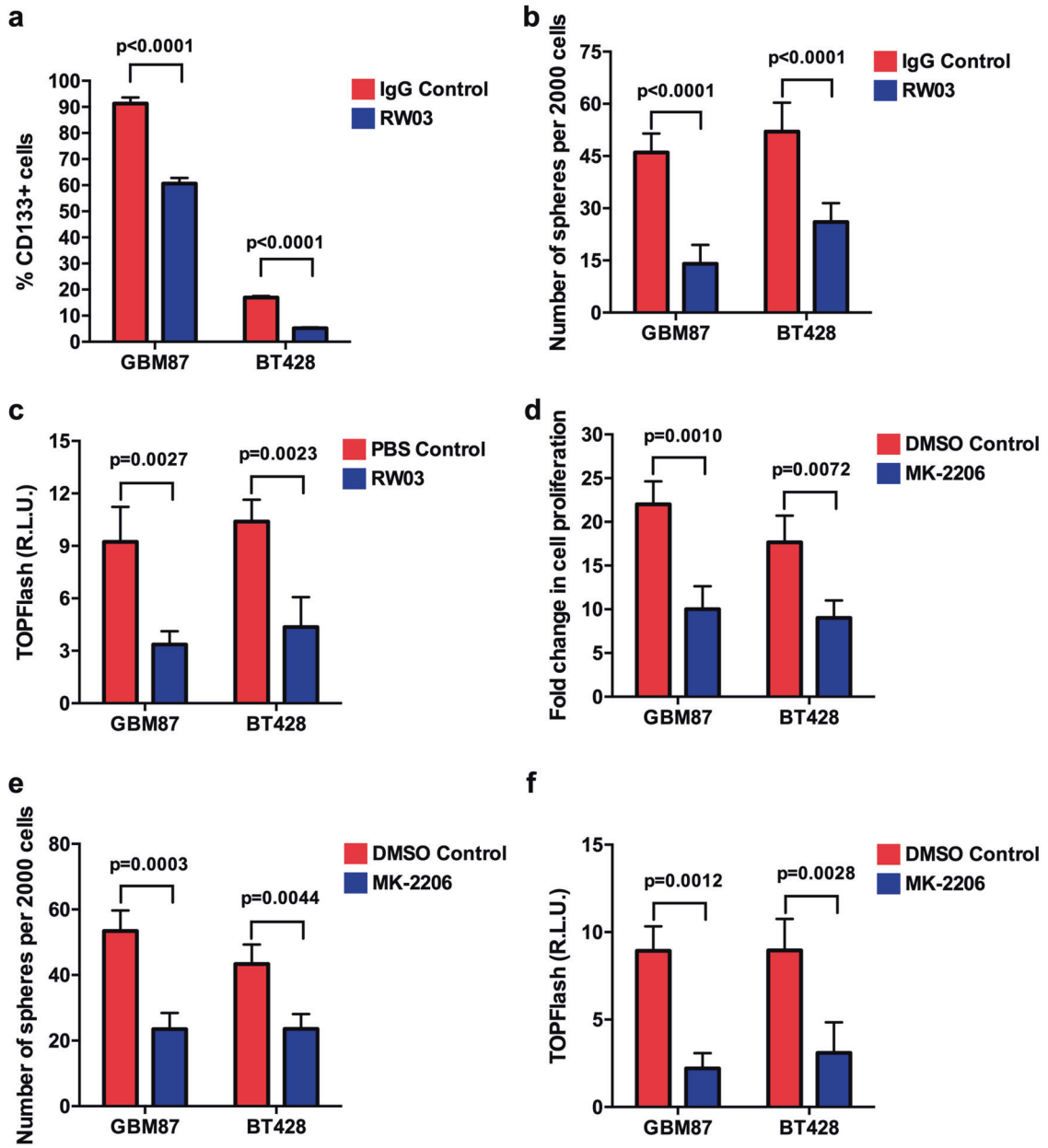

Fig. 3 Upstream inhibition of CD133 or AKT impairs downstream Wnt activity. Treatment of CD133^{high} GBM lines, GBM87 and BT428, with the CD133 monoclonal antibody RW03 (50 nM) reduces **a** surface CD133 expression (GBM87: $p < 0.0001$, BT428: $p < 0.0001$) ($n = 3$, independent experiments per GBM line), **b** self-renewal potential (GBM87: $p < 0.0001$, BT428: $p < 0.001$), and **c** TCF reporter activity (GBM87: $p = 0.0027$, BT428: $p = 0.0023$) ($n = 3$, independent experiments per GBM line). AKT inhibition using the small molecule MK-2206 (5uM), significantly reduces **d** proliferation (GBM87: $p = 0.0010$, BT428: $p = 0.0072$), **e** self-renewal (GBM87: $p = 0.0003$, BT428: $p = 0.0044$), and **f** TCF reporter activity (GBM87: $p = 0.0012$, BT428: $p = 0.0028$) in CD133^{high} GBM cells when compared with control ($n = 3$, independent experiments per GBM line)

using flow cytometric cell sorting (Supplementary Fig. 6b). The enhanced Wnt activity in TGP+ cells compared with TGP− cells was validated with the TCF Wnt reporter assay (Fig. 4a). In vitro functional characterization of TGP+ and TGP− cells demonstrated a significant increase in the proliferative (Fig. 4b) and self-renewal (Fig. 4c) capacity of TGP + compared with TGP− cells. To determine if the observed differences in in vitro functional assays may be in part due to an AKT-dependent activation of the Wnt signaling pathway in TGP+ cells, we assessed the protein levels of pAKT (Ser473), pGSK (Ser9), and β-catenin in TGP+ and TGP− cells (Fig. 4d). Given that all proteins were enriched in TGP+ cells when compared with TGP− cells, our analysis confirmed the role of this novel signaling cascade in regulating

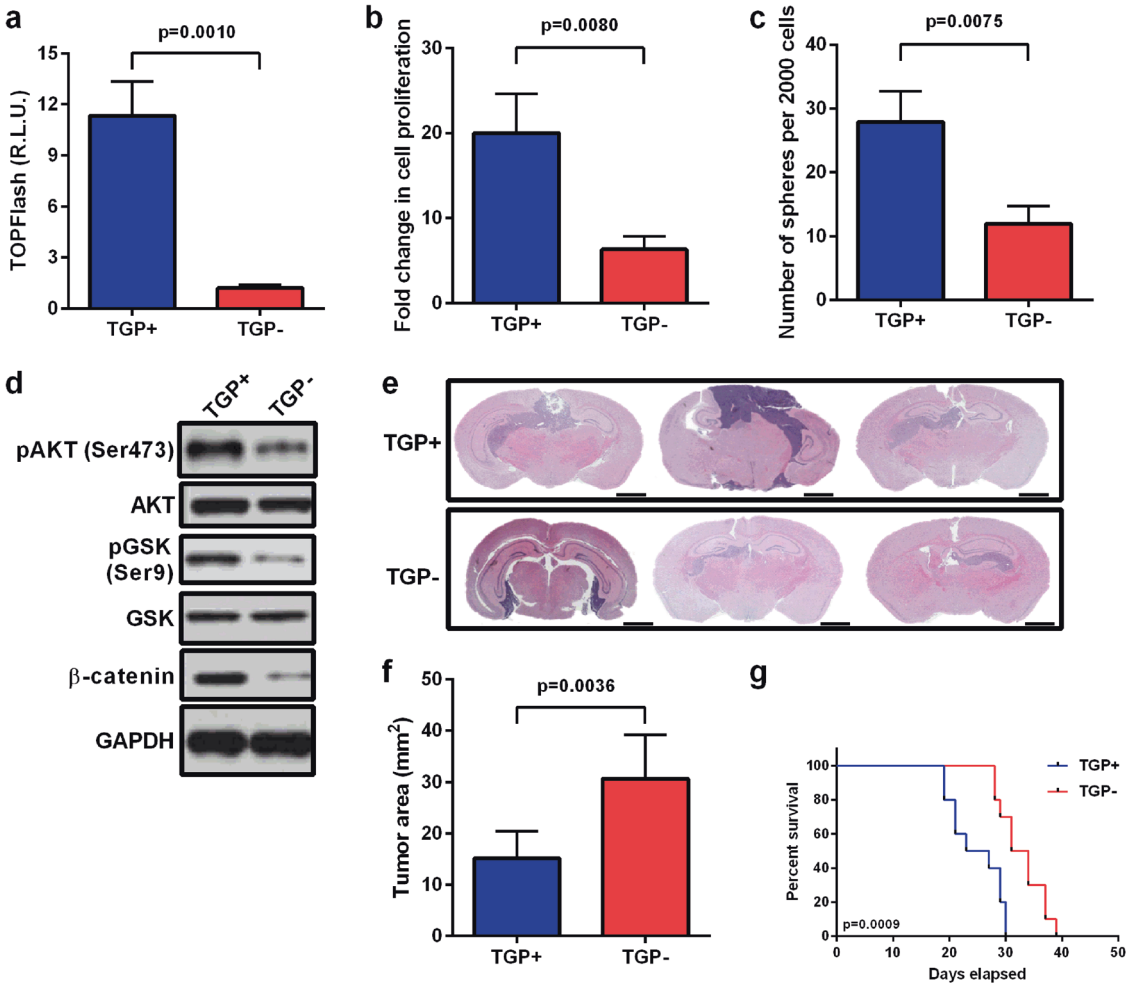

Fig. 4 Endogenous Wnt active BT241 GBM cells display enhanced tumorigeneicity. **a** TGP+ cells contain enhanced TCF reporter activity when compared with TGP− cells ($p = 0.0010$) ($n = 3$, independent experiments). **b** Proliferative ($p = 0.0080$) and **c** self-renewal capacity ($p = 0.0075$) of TGP+ cells are significantly increased when compared with TGP− cells ($n = 3$, independent experiments). **d** Protein levels of putative CD133-AKT-Wnt signaling axis indicating an increase in pAKT, pGSK, and β-catenin in TGP+ cells compared with TGP− cells ($n = 1$). **e** Representative histology images illustrating increased tumor burden in TGP+ ($n = 10$) compared with TGP− xenografts ($n = 10$). **f** Xenografts generated from TGP+ cells ($n = 10$) contain larger tumor volumes when compared with TGP− xenografts ($n = 10$) ($p = 0.0036$). **g** TGP+ xenografts ($n = 10$, median survival 25.0 days) display a significant decrease in overall survival when compared with TGP− xenografts ($n = 10$, median survival 32.5 days) ($p = 0.0009$). Histology image scale bar = 5000 μm

Wnt activity and further illustrated how this pathway may contribute to intratumoral heterogeneity at the protein level in GBM. We then assessed the tumor-initiating capacity of TGP + and TGP− cells and wondered if TGP+ cells formed more aggressive tumors in vivo. Xenografts were generated with orthotopic injections of TGP+ or TGP− cells. Overall tumor burden was increased in TGP+ xenografts compared with mice with TGP− cells (Fig. 4e, f). A reduced survival advantage was also seen in TGP+ xenografts, which had a median survival of 25.0 days compared with 32.5 days in TGP− xenografts (Fig. 4g). These data highlight the functional significance of a signaling nexus in which CD133 enhances Wnt pathway expression through AKT and further illustrate the importance of addressing the proteomic heterogeneity that may further contribute to treatment failure and poor patient outcome in GBM.

Discussion

The advent of molecular diagnostics and large-scale integrated genomic analyses of tumors have reconceptualized our understanding of the biology of many cancers, including GBM [9, 27, 28]. While these studies have uncovered several actionable therapeutic targets, their clinical utility has been inadequate with no improvements in overall survivorship [34, 35]. This may in part be due to the limited efficacy of monotherapy trials and our poor understanding of cross-talk

and convergence among cell signaling pathways [34–36]. The identification of context-specific signaling mechanisms as in the case of AKT-mediated activation of Wnt signaling may have therapeutic implications as downstream pathways may converge on common nodes of integration, which may be missed by current integrated genomics that lack corresponding proteomic data [36].

Insight into the function of CD133 has been limited to the discovery of a single-nucleotide frameshift mutation in the *CD133* gene, leading to an autosomal-recessive retinal degenerative disease [37]. While these findings establish a role for CD133 in retinal development, they have not been carried forward into identifying the functional significance of CD133 in oncology. Through functioning as a cell surface marker for TIC populations that have been shown to interact with the PI3K/AKT pathway [10], CD133 may be a novel cell surface receptor for several oncogenic pathways that converge on common signaling nodes of interaction. Although the pool of GSK-3 phosphorylated by activated AKT has historically not been associated with Wnt/β-catenin signaling [38], emerging data have implicated an alternative pathway by which AKT may activate the Wnt/β-catenin pathway [39]. Earlier work has indicated growth factor signaling through AKT to phosphorylate GSK-3 and thereby inhibit substrate accessibility to GSK-3. The subsequent stabilization of substrates normally phosphorylated by GSK-3 remains controversial and context-dependent [40]. One determining factor for when AKT may not stabilize GSK-3 substrates may be in the presence of activating mutations in components of GSK-3-mediated pathways [38]. In contrast, since recurrent mutations of the Wnt/β-catenin pathway have not been identified in GBM, AKT may stabilize and enhance β-catenin expression to maintain developmental signaling programs in BTIC populations.

By modulating CD133, AKT, and Wnt/β-catenin with a variety of targeted approaches, we have provided evidence in support of a CD133-AKT-Wnt pathway in human GBM. Specifically, this work illustrates an emerging paradigm in Wnt biology in which functions of the pathway may be elicited by non-canonical receptors and upstream activators. Using our TIC models, we have validated the clinical relevance of this pathway in its ability to drive GBM growth and lead to poor overall survivorship. The identification of GBM cells with endogenous Wnt activity having enhanced expression of our signaling axis further signifies the importance of clonal dynamics and the advantages of single-cell proteomics when functionally interrogating heterogeneous cell populations for unique vulnerabilities. As molecularly-based clinical oncology trials continue to expand, novel approaches to overcome the dependence of tumors on malignant pathways are warranted such that common nodes of interaction within divergent cell signaling pathways may be targeted by multiple treatment modalities.

Materials and methods

Culture of primary GBM samples

Primary human GBMs (Supplementary Table 1) and whole 13- or 14-week fetal brain samples were obtained from consenting patients and families as approved by the Hamilton Health Sciences/McMaster Health Sciences Research Ethics Board. Samples were dissociated in PBS containing 0.2 Wünsch unit/mL of Liberase Blendzyme 3 (Roche), and incubated at 37 °C in a shaker for 15 min. The dissociated tissue was filtered through a 70 µm cell strainer and collected by centrifugation (1500 rpm, 3 min). GBM87 was a kind gift from Dr. Hiroaki Wakimoto (Massachusetts General Hospital, Boston, MA, USA). Tumor cells and human NSCs (hNSCs) from fetal brain were resuspended in a serum-free brain tumor-initiating cell (BTIC) enrichment media, and replated on ultra-low attachment plates (Corning). BTIC enrichment media was composed of NeuroCult complete media (StemCell Technologies), 10 ng/mL bFGF, 20 ng/mL EGF, and 2 µg/mL heparin.

Flow cytometric analysis and cell-sorting

Tumorspheres were dissociated and single cells resuspended in PBS +2 mmol/L EDTA. For total (internal and surface) characterization of CD133 levels, cells were fixed using Fixation/Permeabilization Solution Kit (BD). Cells were stained with APC-conjugated anti-CD133 or a matched isotype control (Miltenyi) and incubated for 30–40 min on ice. Samples were run on a MoFlo XDP Cell Sorter (Beckman Coulter). Dead cells were excluded using the viability dye 7AAD (1:10, Beckman Coulter) or using a near IR Live/Dead fixable staining kit (Life Technologies). Compensation was performed using mouse IgG CompBeads (BD). CD133 or GFP expression (for endogenous Wnt active cells) were defined as positive or negative based on the analysis regions set on the isotype control or untransduced cells respectively. GFP+ and GFP− cells were sorted into tubes containing 1 mL BTIC enrichment media and small aliquots of each sort tube were analyzed to determine the purity of the sorted populations. Cells were allowed to equilibrate at 37 °C for a few hours prior to experimentation.

Wnt/TCF reporter assay

GBM cells were cotransfected with the constructs 8XTOPFlash (1.8 mg), driving firefly luciferase, and pRL-CMV (0.2 mg), driving the expression of Renilla luciferase for normalization (Promega). After 24 h, GBM cells were supplemented with BTIC enrichment medium. Cells were washed twice with PBS 24 h following medium change and were lysed with passive lysis buffer (Promega). The luciferase reporter activities were

measured using a luminometer as per the manufacturer's instructions (Promega Dual-Light System).

Quantitative real-time polymerase chain reaction

Total RNA was extracted using the Norgen Total RNA isolation kit and quantified using a NanoDrop Spectrophotometer ND-1000. Complementary DNA was synthesized from 0.5–1 µg RNA using the qScript cDNA Super Mix (Quanta Biosciences) and a C1000 Thermo Cycler (Bio-Rad) with the following cycle parameters: 4 min at 25 °C, 30 min at 42 °C, 5 min at 85 °C, hold at 4 °C. qRT-PCR was performed using the Perfecta SybrGreen (Quanta Biosciences) and CFX96 instrument (Bio-Rad). CFX Manager 3.0 software was used for quantification of gene expression and levels were normalized to GAPDH expression with secondary validation normalized to Actin expression. Primers include: *Actin* (F: 5'-TATCCCTGTA CGCCTCT-3'; R: 5'-AGGTCTTTGCGGATGT-3'), *Axin2* (F: 5'-TGGAGCCGGCTGCGCTTTGAT-3'; R: 5'-CTGG GGTCCGGGAGGCAAGTC-3'), *GAPDH* (F: 5'-TGCA CCACCAACTGCTTAGC-3'; R: 5'-GGCATGGACTGT GGTCATGAG-3').

Lentiviral studies

OE-Ctrl and OE-CD133 vectors were purchased from Genecopoeia. TGP endogenous canonical Wnt reporter (8X TOPFlash TCF reporter) (#24305) was purchased from Addgene. Replication-incompetent lentiviruses were produced by cotransfection of the expression vector and packaging vectors pMD2G and psPAX2 in HEK293FT cells. Viral supernatants were harvested 72 h after transfection, filtered through a 0.45 µm cellulose acetate filter, and precipitated with PEGit (System Biosciences). The viral pellet was resuspended in 1.0 mL of DMEM media and stored at −80 °C. Stable cell lines were generated by transduction followed by maintenance of cultures with puromycin or flow cytometric cell sorting for GFP+ and GFP− cells.

Cell proliferation assay

Single cells were plated in 96-well plates, at a density of 1000 cells/200 µL per well in quadruplicate for each sample and incubated for four days. 20 µL of Preso Blue (Life Technologies), a fluorescent cell metabolism indicator, was added to each well ~4 h prior to the readout time point. Fluorescence was measured with a FLUOstar Omega Fluorescence 556 Microplate reader (BMG LABTECH) at an excitation and emission wavelength of 540 and 570 nm, respectively. Readings were analyzed using the Omega software.

Self-renewal analysis

GBM BTIC tumorspheres were mechanically dissociated with a 1000 µL pipette tip or enzymatically disassociated using Liberase (Roche) and DNase. To conduct a secondary sphere formation assay, cells were plated at 200 cells per well in 200 µL of BTIC enrichment media in a 96-well plate. Cultures were left undisturbed at 37 °C with 5% CO_2. After 3 days, number of secondary spheres per well was counted and used to estimate the mean number of spheres/2000 cells. To conduct a limiting dilution assay, dissociated cells were plated at dilutions from 512 to 2 cells per well. After 7 days, the absence or presence of secondary spheres in each well was noted and used to determine stem cell frequency [41].

Western immunoblotting

Denatured total protein (10 µg) was separated using 10% sodium dodecyl sulphate-polyacrylamide gel electrophoresis and transferred to polyvinylidene fluoride membrane. Western blots were probed with the following primary antibodies: AKT (rabbit; 1:1000; Cell Signaling #4691), pAKT (mouse; 1:1000; Cell Signaling #4051), β-catenin (mouse; 1:10,000; BD Biosciences #610154), GSK-3 (mouse; 1:2000; Sigma #44–610), pGSK-3β-Ser9 (rabbit; 1:1000; Cell Signaling #5558), GAPDH (mouse; 1:50,000; Abcam #ab8245), and βtub (rabbit; 1/500; Abcam #ab6046). The secondary antibody was horseradish peroxidase-conjugated goat anti-mouse IgG (Bio-Rad). The bands were visualized using an Immobilon Western kit (Millipore) and Chemidoc.

Small molecule inhibitors

The CD133 monoclonal antibody, RW03, developed by our collaborator Dr. Jason Moffat (University of Toronto) was used to inhibit CD133 signaling at the receptor level. GBM BTICs were treated with RW03 at concentrations of 10, 25, and 50 nM. PBS or control IgG were used as control. Changes in endogenous Wnt activity were then assessed using the Wnt/TCF reporter assay. Wnt signaling was inhibited using XAV939 at a concentration of 1 µM. DMSO was used as a control. The pan-AKT inhibitor, MK-2206 was used to inhibit AKT signaling at concentrations of 1, 5, 10 µM. DMSO was used as a control. Functional assays (proliferation, self-renewal) and Wnt/TCF reporter assays were performed on pretreated GBM BTICs using 50 nM RW03 and 5 µM MK-2206. Treatments were not maintained for the length of the assay.

In vivo experiments

All in vivo studies were performed according to McMaster University Animal Research Ethics Board

approved protocols. Intracranial injections were performed as previously described [6] using human GBM BT241. Briefly, the appropriate number of live cells determined by Trypan Blue exclusion were resuspended in 10 µL of PBS. NOD-SCID mice were anaesthetized using isofluorane gas (5% induction, 2.5% maintenance) and cells were injected into the frontal lobe using a 10 µL Hamilton syringe. Tumor-initiating capacity, histological differences in tumor size, and survival analysis of BT241 TGP+ (endogenous Wnt active cells, $n = 10$) compared with BT241 TGP− (endogenous Wnt inactive cells, $n = 10$) were performed using 5 mice per dilution at dilutions of 1.0×10^5 and 5.0×10^4. All mice were sacrificed at endpoint, brains were harvested, formalin-fixed, and paraffin-embedded for hematoxylin and eosin (H&E) staining. The sample size was determined based on prior experiments, which yielded significant differences in survival and tumor size. Mice were randomly selected for injected cell type but investigators were not blinded to treatment group. Images were taken using the Aperio Slide Scanner and analyzed using ImageScope v11.1.2.760 software (Aperio). Tumor volume was assessed using the area of tumor present on 4–6 coronal sections of the mouse brains stained with H&E. Given the heterogeneity in the location and pattern of tumor growth as some lesions tracked in the ventricular and extra-parenchymal spaces rather than invasively through the brain, our tumor volume analysis is a gross approximation but reliably trends with in vivo survival analysis.

Statistical analysis

At least three biological replicates were performed for each experiment. Data represent mean ± standard error (mean) with n values listed in figure legends. Student's t-test analyses were performed using GraphPad Prism™ with significance set to $P < 0.05$. Kaplan–Meier survival curves were visualized using GraphPad Prism™.

Acknowledgements B.M. is supported by a Canadian Institutes of Health Research Vanier Canada Graduate Scholarship. S.K.S. is supported by the Neurosurgical Research and Education Foundation and American Association of Neurological surgeons, Pediatric Section, the Ontario Institute for Cancer Research, and McMaster University Department of Surgery.

Author contributions BM, CV, CC, BWD, SKS conceptualized and designed the experiments. BM, CV, CC, MS, NS, NT performed experiments and acquired data. BM, CV, CC, BWD, SKS analyzed and interpreted data. BM wrote the manuscript with revisions contributed by CV, CC, BWD, and SKS. JM provided non-commercial reagents. JPP, NKK provided GBM study samples. BWD and SKS supervised the study. All authors reviewed results and commented on the manuscript.

Compliance with ethical standards

Conflict of interest The authors declare that they have no conflict of interest.

Publisher's note Springer Nature remains neutral with regard to jurisdictional claims in published maps and institutional affiliations.

References

1. Yin AH, Miraglia S, Zanjani ED, Almeida-Porada G, Ogawa M, Leary AG, et al. AC133, a novel marker for human hematopoietic stem and progenitor cells. Blood. 1997;90:5002–12.
2. Uchida N, Buck DW, He D, Reitsma MJ, Masek M, Phan TV, et al. Direct isolation of human central nervous system stem cells. Proc Natl Acad Sci USA. 2000;97:14720–5.
3. Cox CV, Diamanti P, Evely RS, Kearns PR, Blair A. Expression of CD133 on leukemia-initiating cells in childhood ALL. Blood. 2009;113:3287–96.
4. Hermann PC, Huber SL, Herrler T, Aicher A, Ellwart JW, Guba M, et al. Distinct populations of cancer stem cells determine tumor growth and metastatic activity in human pancreatic cancer. Cell Stem Cell. 2007;1:313–23.
5. O'Brien CA, Pollett A, Gallinger S, Dick JE. A human colon cancer cell capable of initiating tumour growth in immunodeficient mice. Nature. 2007;445:106–10.
6. Singh SK, Hawkins C, Clarke ID, Squire JA, Bayani J, Hide T, et al. Identification of human brain tumour initiating cells. Nature. 2004;432:396–401.
7. Shibahara I, Sonoda Y, Saito R, Kanamori M, Yamashita Y, Kumabe T, et al. The expression status of CD133 is associated with the pattern and timing of primary glioblastoma recurrence. Neuro-Oncol. 2013;15:1151–9.
8. Zeppernick F, Ahmadi R, Campos B, Dictus C, Helmke BM, Becker N, et al. Stem cell marker CD133 affects clinical outcome in glioma patients. Clin Cancer Res. 2008;14:123–9.
9. Verhaak RG, Hoadley KA, Purdom E, Wang V, Qi Y, Wilkerson MD, et al. Integrated genomic analysis identifies clinically relevant subtypes of glioblastoma characterized by abnormalities in PDGFRA, IDH1, EGFR, and NF1. Cancer cell. 2010;17:98–110.
10. Wei Y, Jiang Y, Zou F, Liu Y, Wang S, Xu N, et al. Activation of PI3K/Akt pathway by CD133-p85 interaction promotes tumorigenic capacity of glioma stem cells. Proc Natl Acad Sci USA. 2013;110:6829–34.
11. Chenn A, Walsh CA. Regulation of cerebral cortical size by control of cell cycle exit in neural precursors. Science. 2002;297:365–9.
12. Kim WY, Wang X, Wu Y, Doble BW, Patel S, Woodgett JR, et al. GSK-3 is a master regulator of neural progenitor homeostasis. Nat Neurosci. 2009;12:1390–7.
13. Rossi M, Magnoni L, Miracco C, Mori E, Tosi P, Pirtoli L, et al. beta-catenin and Gli1 are prognostic markers in glioblastoma. Cancer Biol Ther. 2011;11:753–61.
14. Zhang LY, Jiang LN, Li FF, Li H, Liu F, Gu Y, et al. Reduced beta-catenin expression is associated with good prognosis in Astrocytoma. Pathol Oncol Res. 2010;16:253–7.
15. Mak AB, Nixon AM, Kittanakom S, Stewart JM, Chen GI, Curak J, et al. Regulation of CD133 by HDAC6 promotes beta-catenin signaling to suppress cancer cell differentiation. Cell Rep. 2012;2:951–63.
16. Morin PJ, Sparks AB, Korinek V, Barker N, Clevers H, Vogelstein B, et al. Activation of beta-catenin-Tcf signaling in colon cancer by mutations in beta-catenin or APC. Science. 1997;275:1787–90.

17. Brennan CW, Verhaak RG, McKenna A, Campos B, Noushmehr H, Salama SR, et al. The somatic genomic landscape of glioblastoma. Cell. 2013;155:462–77.
18. Hu B, Wang Q, Wang YA, Hua S, Sauve CG, Ong D, et al. Epigenetic activation of WNT5A drives glioblastoma stem cell differentiation and invasive growth. Cell. 2016;167:1281–1295 e1218.
19. Ji H, Wang J, Nika H, Hawke D, Keezer S, Ge Q, et al. EGF-induced ERK activation promotes CK2-mediated disassociation of alpha-Catenin from beta-Catenin and transactivation of beta-Catenin. Mol cell. 2009;36:547–59.
20. Morris LG, Kaufman AM, Gong Y, Ramaswami D, Walsh LA, Turcan S, et al. Recurrent somatic mutation of FAT1 in multiple human cancers leads to aberrant Wnt activation. Nat Genet. 2013;45:253–61.
21. Pulvirenti T, Van Der Heijden M, Droms LA, Huse JT, Tabar V, Hall A. Dishevelled 2 signaling promotes self-renewal and tumorigenicity in human gliomas. Cancer Res. 2011;71:7280–90.
22. Rheinbay E, Suva ML, Gillespie SM, Wakimoto H, Patel AP, Shahid M, et al. An aberrant transcription factor network essential for Wnt signaling and stem cell maintenance in glioblastoma. Cell Rep. 2013;3:1567–79.
23. Yang W, Xia Y, Ji H, Zheng Y, Liang J, Huang W, et al. Nuclear PKM2 regulates beta-catenin transactivation upon EGFR activation. Nature. 2011;480:118–22.
24. Zhang N, Wei P, Gong A, Chiu WT, Lee HT, Colman H, et al. FoxM1 promotes beta-catenin nuclear localization and controls Wnt target-gene expression and glioma tumorigenesis. Cancer Cell. 2011;20:427–42.
25. Zheng H, Ying H, Wiedemeyer R, Yan H, Quayle SN, Ivanova EV, et al. PLAGL2 regulates Wnt signaling to impede differentiation in neural stem cells and gliomas. Cancer Cell. 2010;17:497–509.
26. Sastre-Perona A, Riesco-Eizaguirre G, Zaballos MA, Santisteban P. beta-catenin signaling is required for RAS-driven thyroid cancer through PI3K activation. Oncotarget. 2016;7:49435–49.
27. Lan X, Jorg DJ, Cavalli FMG, Richards LM, Nguyen LV, Vanner RJ, et al. Fate mapping of human glioblastoma reveals an invariant stem cell hierarchy. Nature. 2017;549:227–32.
28. Patel AP, Tirosh I, Trombetta JJ, Shalek AK, Gillespie SM, Wakimoto H, et al. Single-cell RNA-seq highlights intratumoral heterogeneity in primary glioblastoma. Science. 2014;344:1396–401.
29. Hambardzumyan D, Squatrito M, Carbajal E, Holland EC. Glioma formation, cancer stem cells, and akt signaling. Stem Cell Rev. 2008;4:203–10.
30. Holland EC, Celestino J, Dai C, Schaefer L, Sawaya RE, Fuller GN. Combined activation of Ras and Akt in neural progenitors induces glioblastoma formation in mice. Nat Genet. 2000;25:55–7.
31. Uhrbom L, Dai C, Celestino JC, Rosenblum MK, Fuller GN, Holland EC. Ink4a-Arf loss cooperates with KRas activation in astrocytes and neural progenitors to generate glioblastomas of various morphologies depending on activated Akt. Cancer Res. 2002;62:5551–8.
32. ter Haar E, Coll JT, Austen DA, Hsiao HM, Swenson L, Jain J. Structure of GSK3beta reveals a primed phosphorylation mechanism. Nat Struct Biol. 2001;8:593–6.
33. Fuerer C, Nusse R. Lentiviral vectors to probe and manipulate the Wnt signaling pathway. PLoS ONE 2010;5:e9370.
34. Taal W, Oosterkamp HM, Walenkamp AM, Dubbink HJ, Beerepoot LV, Hanse MC, et al. Single-agent bevacizumab or lomustine versus a combination of bevacizumab plus lomustine in patients with recurrent glioblastoma (BELOB trial): a randomised controlled phase 2 trial. Lancet Oncol. 2014;15:943–53.
35. Weller M, Butowski N, Tran DD, Recht LD, Lim M, Hirte H, et al. Rindopepimut with temozolomide for patients with newly diagnosed, EGFRvIII-expressing glioblastoma (ACT IV): a randomised, double-blind, international phase 3 trial. Lancet Oncol. 2017;18:1373–85.
36. Wei W, Shin YS, Xue M, Matsutani T, Masui K, Yang H, et al. Single-cell phosphoproteomics resolves adaptive signaling dynamics and informs targeted combination therapy in glioblastoma. Cancer Cell. 2016;29:563–73.
37. Maw MA, Corbeil D, Koch J, Hellwig A, Wilson-Wheeler JC, Bridges RJ, et al. A frameshift mutation in prominin (mouse)-like 1 causes human retinal degeneration. Hum Mol Genet. 2000;9:27–34.
38. Ng SS, Mahmoudi T, Danenberg E, Bejaoui I, de Lau W, Korswagen HC, et al. Phosphatidylinositol 3-kinase signaling does not activate the wnt cascade. J Biol Chem. 2009;284:35308–13.
39. Fukumoto S, Hsieh CM, Maemura K, Layne MD, Yet SF, Lee KH, et al. Akt participation in the Wnt signaling pathway through Dishevelled. J Biol Chem. 2001;276:17479–83.
40. Manning BD, Toker A. AKT/PKB signaling: navigating the network. Cell. 2017;169:381–405.
41. Singh SK, Clarke ID, Terasaki M, Bonn VE, Hawkins C, Squire J, et al. Identification of a cancer stem cell in human brain tumors. Cancer Res. 2003;63:5821–8.